https://doi.org/10.22226/2410-3535-2022-2-158-163

Influence of technological parameters on the process of SHS-extrusion of composite material $MgAl_2O_4$-TiB_2

A. P. Chizhikov†, A. S. Konstantinov, P. M. Bazhin, M. S. Antipov

†chij@ism.ac.ru

Merzhanov Institute of Structural Macrokinetics and Materials Science, RAS, Chernogolovka, 142432, Russia

Ceramic rods based on $MgAl_2O_4$-TiB_2 material were obtained by SHS-extrusion. The effect of technological parameters (delay time before applying pressure, deformation rate, molding pressure) and design parameters on the process of SHS extrusion of the material, as well as the structure and phase composition of the obtained products, were studied. Ceramic hollow rods based on aluminum-magnesium spinel and titanium diboride up to 100 mm long and with an outer diameter of 5, 6, and 7 mm were obtained. It has been established that the deformation rate has the greatest influence on the process of SHS extrusion of the studied material. It is shown that changing the value of this parameter makes it possible to obtain both compact and hollow rods. The resulting hollow rods had a composite structure: the basis of the rods was octahedral grains characteristic of spinel, 10 – 40 μm in size. Cubic grains of titanium diboride were distributed over the entire volume of the obtained hollow rods and had a size of less than 1 μm. Compact rods consisted of a core, mainly composed of titanium diboride, which is covered with a shell of magnesium aluminum spinel with a thickness of less than 1 mm.

Keywords: self-propagating high-temperature synthesis, spinel, alumina, SHS-extrusion.

1. Introduction

An urgent task for the modern scientific and technical complex is the development of new promising materials and products based on them. These materials include composites based on oxide ceramics. Oxide ceramic materials are widely used in various industries as cutting ceramics [1–3], refractory materials [4,5], protective coatings [6,7], as materials for fuel cells [8,9], etc. Among a wide range of oxide ceramic materials, materials based on magnesium aluminum spinel $MgAl_2O_4$ can be singled out. These materials have a high melting point (2135°C), high hardness, high chemical and corrosion resistance to acids and molten metals [10,11]. The described properties make materials based on aluminum-magnesium spinel promising for use in the chemical and metallurgical industries for the manufacture of protective covers for thermocouples, various crucibles and molds, and refractory linings [12–14]. At the same time, the wide introduction of materials based on aluminum-magnesium spinel is hindered due to its low mechanical properties at room and high temperatures [15]. From this point of view, it is promising to create composite materials based on $MgAl_2O_4$ strengthened by particles of the secondary phase. Various oxides [16,17] and carbides [18], borides [19], nitrides [20], etc. [21] can be used as the secondary phase. So in the work of Sun et al. [22] the preparation of a composite refractory material $MgAl_2O_4$-Al_2O_3-Ti (C, N) is made by sintering Al_2O_3, MgO, TiO_2 and Al powders at a temperature of 1500°C in a nitrogen flow. The authors report that the formation of Ti (C, N) particles in the composite improved the refractory properties of the resulting material.

The synthesis of materials based on $MgAl_2O_4$ is complicated due to the fact that the formation of this compound occurs as a result of an endothermic reaction of magnesium and aluminum oxides and requires the use of high temperatures. There are also low-temperature methods for the synthesis of spinels, such as the sol-gel method [23] and hydrothermal synthesis [24]. However, these methods are complicated by the need to process acids, solutions, gels and the intricacy of the equipment. Consolidation and production of finished products from materials based on $MgAl_2O_4$ is complicated due to the high melting point of such materials and the intricacy of their processing. Basically, for these purposes, varieties of spark plasma sintering [25], hot pressing, and other methods of powder metallurgy [26] are used. In the work of Liu and Morita [27], compact samples of the $MgAl_2O_4$-Al_2O_3 material were obtained by the SPS method, while the porosity of the obtained samples was less than 1%. Marais et al. [25] describe the possibility of obtaining compact workpieces based on $MgAl_2O_4$-Al_2O_3 by reactive spark sintering by introducing stabilized ZrO_2 (8YSZ), which has ionic conductivity, into the system. In their study, Liu et al. [28] report the prospect of using a combination of microwave sintering and hot isostatic pressing. The authors report that the use of such a combination made it possible both to obtain samples with a high relative density (95.4%) and to significantly reduce the process time compared to conventional sintering. These methods are widely used in modern industry due to their advantages, but there are some limitations to their use. They are associated with the use of complex technological equipment, the need to use external sources of heating, the duration of the process, as well as restrictions on the size of the resulting products.

A promising approach to obtaining products from composite materials based on aluminum-magnesium spinel is a combination of self-propagating high-temperature synthesis (SHS) and shear plastic deformation [29]. The process of SHS occurs due to the release of internal heat of the system during the chemical reaction between the components and is characterized by high process temperatures (>1800°C). This makes it possible to carry out the synthesis of refractory compounds without the use of external heating sources. Lv et al. [30] in their work describe the preparation of the $MgAl_2O_4/C$ composite powder by the SHS method and the use of $MgC_2O_4 \cdot 2H_2O$, MgO_2, Al_2O_3, and Al powders as initial reactants. The authors report that the resulting powder was distinguished by high purity and a uniform distribution of the chemical composition.

At the same time, since the synthesis products are in a heated state, this makes it possible to form finished products by shear plastic deformation. This combination of SHS and shear plastic deformation is implemented in the methods of unrestricted SHS-compression [31] and SHS-extrusion [32]. The SHS-extrusion method makes it possible to obtain finished products from initial powders in one technological stage. Also, in SHS extrusion, there is no need to use external heating, since the energy of the exothermic chemical reaction is used.

Among the articles of other authors, we can note works [33, 34], which describe a process similar to SHS extrusion. In these works, a reaction between the components of the mixture was initiated by external heating, after which external pressure was applied and extrusion was carried out. Mixtures of nickel, aluminum, titanium and iron powders were used as objects of study to obtain intermetallic compounds. However, the samples obtained had a short length and poor surface quality; these works did not receive further serious development. In [35], a similar process is described, but a metal-ceramic composite based on Al_2O_3/Cu-Al was used as the object of study. In this work, external heating of initial samples was also used. Materials with a plastic bond were used as objects of study in these works, which greatly facilitates the extrusion process compared to ceramic samples. The literature describes the extrusion of ceramics [36, 37], including hollow rods [38]. However, in these works, the synthesis of materials due to an exothermic reaction is not used, and the extrusion process itself is carried out on specially prepared suspensions containing a ceramic component. After extrusion, the binding components are removed.

The purpose of this work was the SHS extrusion of a ceramic composite material based on aluminum-magnesium spinel reinforced with titanium diboride particles, as well as the study of the effect of deformation rate on the structure of the resulting products.

2. Materials and methods

Powders of boron oxide (≥99%, <1 μm), aluminum (≥99.5%, <5 μm), magnesium (≥99%, 250 – 450 μm) and titanium (98%, 280 μm) were used as initial reactants in this work. These powders were pre-dried at a temperature of 50°C for 12 hours, after which they were mixed in a ratio of $2B_2O_3$f-2Al-3Mg-2Ti in a drum mill for 12 hours. Next, cylindrical blanks weighing 25 grams and a relative density of 0.65 were prepared from the obtained powder mixture by cold uniaxial pressing. The synthesis of materials was carried out in the SHS mode [39 – 41]. The SHS process occurred due to the reduction of boron oxide with aluminum and magnesium with the formation of the corresponding metal oxides. The reduced boron reacted with titanium to form titanium diboride. Since the formation of spinel occurs with the absorption of heat, the reactions mentioned above, which have a high thermal effect, create favorable conditions for the synthesis of spinel. To obtain products based on the synthesized material, the SHS extrusion method was used, which combines the SHS process and high-temperature shear deformation. The scheme of the SHS-extrusion process is shown in Fig. 1. The extrusion mold consists of a reaction

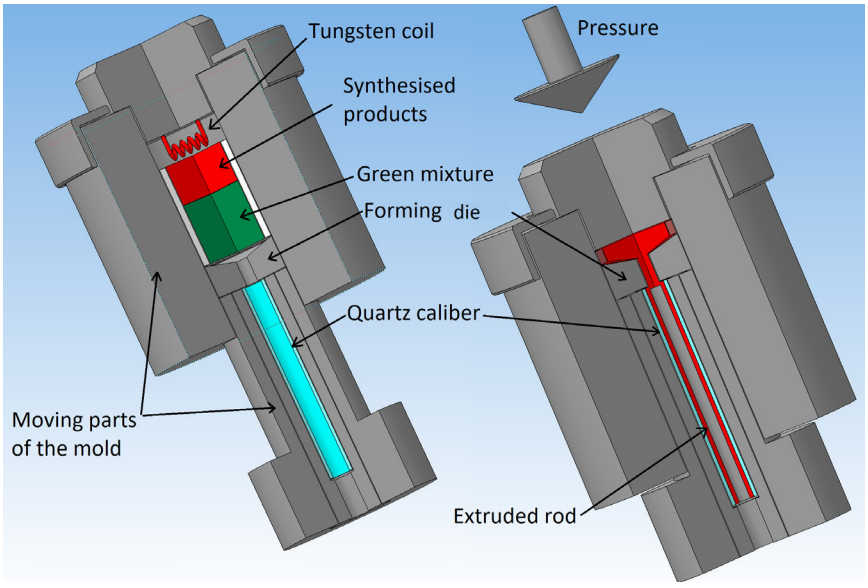

Fig. 1. (Color online) Diagram of the SHS-extrusion process: SHS of the sample in the mold chamber (a), hollow rod in a quartz caliber after extrusion (b).

chamber and a metal cup, in which a quartz guide caliber is placed. Said parts can move freely relative to each other along the pressure application axis. During the experiment, a pre-compressed initial workpiece and a forming die with specified geometric characteristics are placed in the reaction chamber. The SHS process in the mold chamber is initiated by a tungsten spiral, then the combustion wave moves along the sample, and after a certain delay time, external pressure is applied to the sample. Under the action of external pressure, hot synthesis products are squeezed out through the forming die into the guide caliber.

Thermodynamic calculations were carried out using the ISMAN-Thermo software package developed to estimate the probable phase composition of the reaction products, their phase state, and the adiabatic combustion temperature of the system. An experimental study of the combustion temperature was carried out using tungsten-rhenium thermocouples in a setup that simulates the real conditions of SHS extrusion.

The phase composition was studied by X-ray phase analysis (XRD) on a DRON-3M diffractometer. The microstructure of the obtained materials was studied by scanning electron microscopy (SEM) using a Carl Zeiss LEO 1450 VP electron microscope. The results of energy dispersive analysis are given in mass percent.

3. Results and discussion

According to the results of thermodynamic calculations, the adiabatic combustion temperature of the system under study was 2827°C. According to the results of an experimental study of the combustion characteristics of the system under study, the actual combustion temperature was 2127°C. The strong discrepancy between the calculated and experimental results of determining the combustion temperature is explained by the high heat removal that occurs between the sample and the walls of the metal tooling despite the presence of asbestos insulation on the sample.

The combustion temperature significantly exceeded the melting point of the initial components (the most refractory of them is titanium - 1668°C) and aluminum oxide (2072°C) Thus, in the course of synthesis, a liquid phase appears in the material, as a result of which a suspension is formed from liquid initial components, partially liquid synthesis products, and solid particles of synthesis products. The formation of a suspension leads to the fact that the material acquires viscoelastic properties and the ability to plastically deform [42]. Due to the ability to high-temperature plastic deformation, this object of study is promising for the production of products by the SHS-extrusion method. To control the process of SHS-extrusion, there are a number of technological parameters: delay time before applying pressure, deformation rate, molding pressure, as well as design parameters of the forming die.

When establishing the effect of technological and structural parameters on the SHS-extrusion process, ceramic hollow rods based on aluminum-magnesium spinel and titanium diboride up to 100 mm long and with an outer diameter of 5, 6, and 7 mm were obtained. Figure 2 a shows a general view of the fracture of the obtained hollow rods.

One of the most important parameters affecting the SHS extrusion process is the delay time. At low values of this parameter, chemical transformations and structure formation processes are not completed in the material, there is an excess amount of the liquid phase, since in this case the synthesis proceeds with the formation of a sufficiently large amount of the liquid phase. At high values of this parameter, the material undergoes a complete crystallization process, as a result of which the material loses its ability to plastic deformation and extrusion. Thus, there is an optimal delay time interval in which the material has the ability to plastically deform, and also has a sufficient level of viscoelastic properties necessary for the formation of hollow rods. For this material, the optimal delay time was 4 – 5.5 seconds, Fig. 3 a. Another key technological parameter affecting the SHS extrusion of ceramic refractory

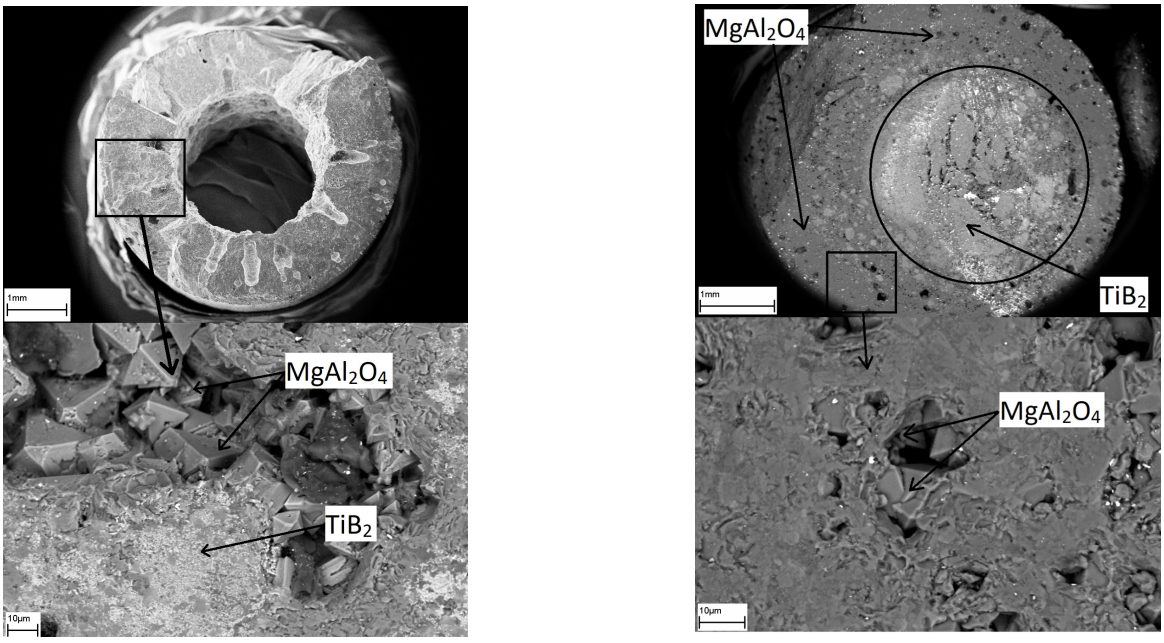

a b

Fig. 2. SEM results of the fracture of the resulting hollow rod (a), of the rod compact obtained at a deformation rate below 65 mm/sec.

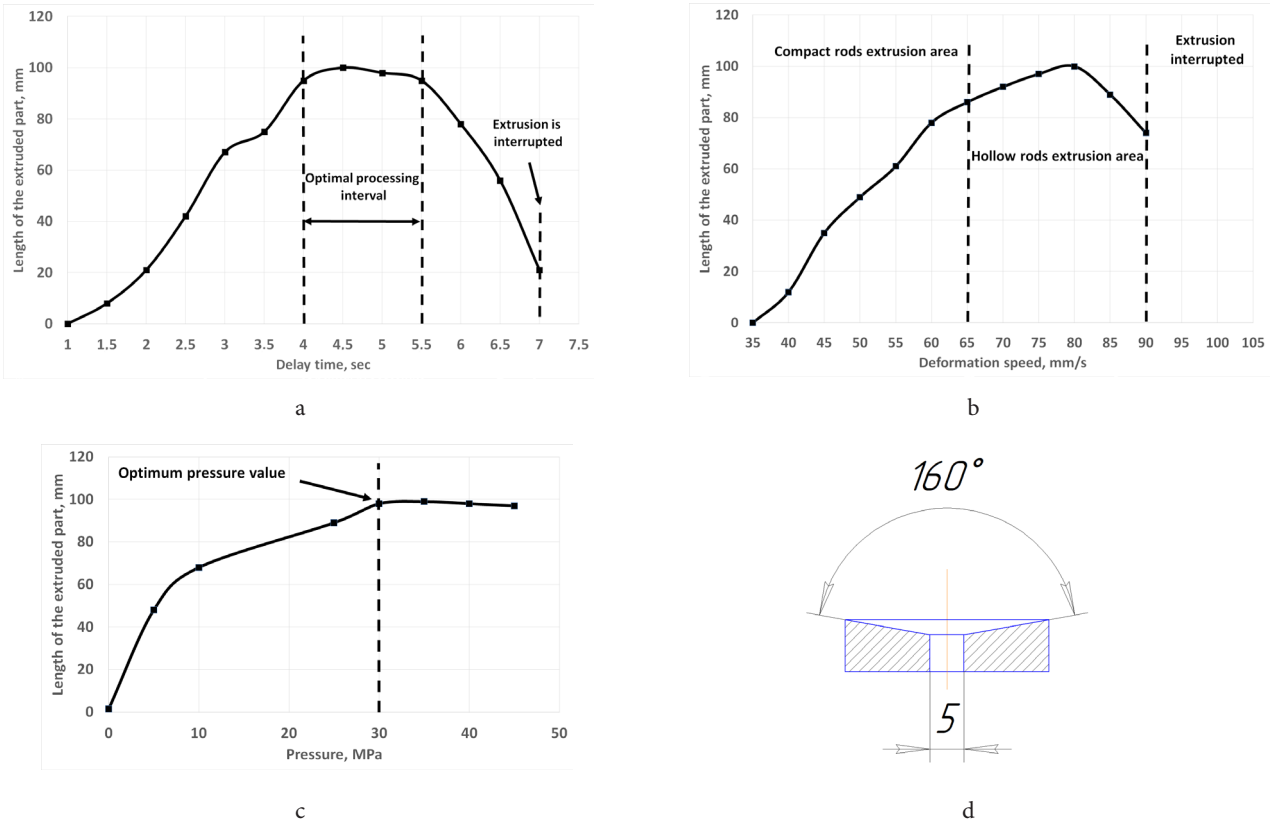

Fig. 3. The dependence of the length of the extruded part on the delay time (a), on the deformation rate (b), on the molding pressure (c), geometric parameters of the forming die (d).

hollow rods is the deformation rate. The "jet swelling" effect (Barus effect) [43,44], which is the basis for the formation of ceramic hollow rods in this work, manifests itself at sufficiently high extrusion rates. In the course of the work, it was found that there is a threshold value of the deformation rate, below which the formation of ceramic hollow rods does not occur. Although the extrusion still occurs. For the studied model composition, such a threshold value was 65 mm/sec, Fig. 3 b. At a lower value of the deformation rate, there is no accumulation of a sufficient amount of elastic strain necessary for the occurrence of normal stresses at the exit from the forming hole, which stretch the material jet. In this case, extrusion occurs in a stationary mode. As a result, based on the studied composition, rods were obtained, which are a compact core, mainly consisting of titanium diboride, which is covered with a shell of aluminum-magnesium spinel with a thickness of less than 1 mm, Fig. 2 b.

In this case, there is also a limiting value of the rate of deformation, above which extrusion does not occur. For the studied model composition, this value was 90 mm/sec. Above this value, the viscosity of the material, which depends on the deformation rate, increases so much that it completely prevents extrusion. Another important technical parameter is the molding pressure. It was found in the work that high molding pressure is not required to obtain ceramic hollow rods. There is a threshold value above which increasing the molding pressure has no effect on the length and quality of the resulting products. For the studied model composition, this value was 30 MPa, Fig. 3 c. This is due to the fact that the viscosity of the studied materials depends more on the extrusion rate than on pressure. Structural parameters also have a great influence on the process of SHS extrusion. So, with a decrease in the angle of the conical part of the die, the contact area of the synthesized material with the die increases, while the magnitude of heat removal increases. As a result, the near-die regions rapidly lose their ability to undergo plastic deformation, and blockage of the exit hole of the die occurs. The optimal value of the angle of the conical part for the studied model composition is 160°. The geometric parameters of the die are shown in Fig. 3 d.

It was shown that by changing the diameter of the exit section of the die, it is possible to obtain hollow rods with different inner diameters. In this case, the outlet of the die must necessarily be less than the diameter of the quartz caliber into which the extrusion is carried out. An important parameter is also the length of the forming channel of the die. With insufficient length during extrusion, there is no sufficient accumulation of elastic strain, as a result of which tensile normal stresses do not arise, and hollow rods do not form. When the optimal value of the length of the forming belt is exceeded, the elastic strain is relaxed directly in the forming channel, which also prevents the formation of ceramic hollow rods. It has been established that an increase in the outer diameter of the obtained ceramic hollow rods due to an increase in the diameter of the quartz caliber, the speed of the press plunger and the mass of the workpiece leads to a decrease in the size of the structural components. This is facilitated by an increase in heat removal that occurs when the material contacts the walls of the quartz caliber. According to the XRD results, the obtained ceramic hollow rods had

a uniform distribution of the phase composition along the entire length. It is also shown that under the conditions of SHS and shear deformation of the studied model composition, the formation of aluminum and magnesium intermetallic compounds occurs. Thus, by adjusting the parameters of SHS extrusion, it is possible to influence the phase composition of the resulting products.

According to the SEM results, Fig. 2 a, the resulting hollow rods had a composite structure. The basis of the rods was octahedral grains characteristic of spinel, 10 – 40 μm in size. Cubic grains of titanium diboride were distributed over the entire volume of the obtained hollow rods and had a size of less than 1 μm. The XRD results showed that the resulting rods mainly consist of two phases: $MgAl_2O_4$ and TiB_2. At the same time, the products also contain traces of unreacted titanium, magnesium oxide, which did not react with Al_2O_3, and $Al_{12}Mg_{17}$ intermetallic compound. The XRD results also showed that the resulting hollow, Fig. 4 a, and compact rods, Fig. 4 b, had a similar phase composition. At the same time, the intensity of the TiB_2 peaks in the compact rod is higher due to its larger amount.

Previously, in [44], the process of SHS extrusion of hollow ceramic rods based on Al_2O_3-CrB was described. In this work, a mechanism was proposed for the formation of hollow rods due to the presence of viscoelastic properties in the reacting mixture. In this paper, the process of SHS extrusion of a composite material based on $MgAl_2O_4$-TiB_2 is described, and the influence of technological parameters on the extrusion process is also studied. In particular, it is shown that the SHS extrusion process of the selected object of study is significantly affected by the deformation rate. It is shown that by changing these parameters it is possible to obtain both hollow and compact ceramic rods.

4. Conclusions

Ceramic rods based on the $MgAl_2O_4$-TiB_2 composite material with a length of more than 100 mm and an outer diameter of 5 – 7 mm were obtained by SHS extrusion. The influence of technological and design parameters on the extrusion process has been studied. It is shown that in order to obtain ceramic hollow rods from this material, there is an optimal temperature-time processing interval in which the material has a sufficient level of viscoelastic properties necessary to obtain hollow rods. It is defined that the deformation rate has a significant effect on the process of extrusion of the specified material. This parameter has a threshold value, for the studied material it was 65 mm/sec, above which hollow rods are formed during extrusion. When extruding at a speed below 65 mm/s, a compact rod is formed, which is a TiB_2-based core in a shell of $MgAl_2O_4$. It was found in the work that high molding pressure is not required to obtain ceramic hollow rods. There is a threshold above which increasing the molding pressure has no effect on the length and quality of the resulting products. For the studied model composition, this value was 30 MPa.

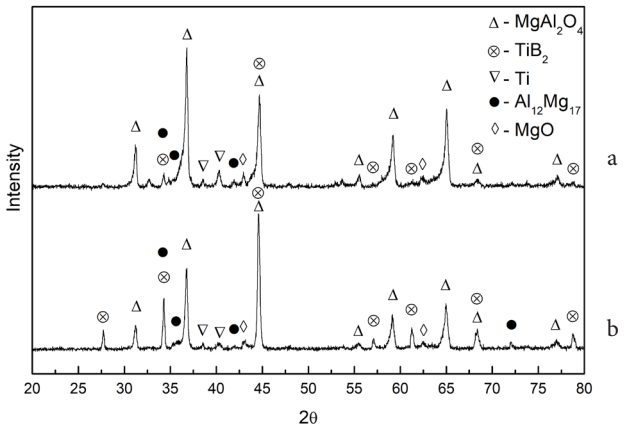

Fig. 4. XRD results of hollow rod (a), of compact rod obtained at a deformation rate below 65 mm/sec (b).

Acknowledgements. This work was supported by the Russian Science Foundation, project no. 20-73-00235.

References

1. X. L. Guo, Z. L. Zhu, M. Ekevad, X. Bao, P. X. Cao. Adv. Appl. Ceram. 117, 16 (2018). Crossref
2. A. I. Pronin, V. V. Myl'nikov, A. A. Rybalkin. Glass Ceram+. 76, 99 (2019). Crossref
3. A. M. Stolin, P. M. Bazhin, A. S. Konstantinov, A. P. Chizhikov, E. V. Kostitsyna, M. Y. Bychkova. Ceram. Int. 44, 13815 (2018). Crossref
4. X. M. Ren, B. Y. Ma, L. L. Wang, G. Q. Liu, J. K. Yu. Ceram. Int. 47, 31130 (2021). Crossref
5. M. Shi, Y. Li, J. J. Shi. Ceram. Int. 48, 7668 (2022). Crossref
6. S. W. Tang, P. F. Liu, Z. Su, Y. Lei, Q. Liu, D. S. Liu. High Temp. Mater. Process. 40, 77 (2021). Crossref
7. I. V. Kozerozhets, G. P. Panasyuk, L. A. Azarova, V. N. Belan, E. A. Semenov, I. L. Voroshilov et al. Theor. Found. Chem. Eng. 55, 1126 (2021). Crossref
8. H. Wang, Z. Lei, H. Zhang, Y. Li, J. Jing, Y. Jin et al. J. Electrochem. Energy Convers. Storage. 19, 011007 (2022). Crossref
9. B. Aktas, S. Tekeli. Arab. J. Geosci. 12, 478 (2019). Crossref
10. I. Ganesh. Int. Mater. Rev. 58, 63 (2013). Crossref
11. Z. Q. Shi, Q. L. Zhao, B. Guo, T. Y. Ji, H. Wang. Mater. Des. 193, 108858 (2020). Crossref
12. J. X. Meng, W. Q. Chen, J. Z. Zhao, L. Liu. High Temp. Mater. Process. 37, 581 (2018). Crossref
13. B. Ma, Y. Yin, Q. Zhu, Y. Zhai, Y. Li, G. Li et al. Refract. Ind. Ceram. 56, 494 (2016). Crossref
14. M. Nguyen, R. Sokolar. Materials. 15, 1363 (2022). Crossref
15. I. Ganesh, J. M. F. Ferreira. Ceram. Int. 35, 259 (2009). Crossref
16. F. Ullah, M. T. Qureshi, K. Sultana, M. Sleem, M. Elaimi, R. A. Hameed et al. Ceram. Int. 47, 20665 (2021). Crossref
17. F. Albanumay, N. Alqahtani, B. Alshammari, H. Alodan, T. Alopily, M. Muhawes. J. Ceram. Process. Res. 21, 683 (2020). Crossref
18. S. H. Alotaibi, Z. I. Zaki. Mater. Res. Express. 6, 105532 (2019). Crossref
19. C. L. Yeh, Y. C. Chen. Crystals. 10, 210 (2020). Crossref
20. A. H. Nassajpour-Esfahani, R. Emadi, A. Alhaji, A. Bahrami, M. R. Haftbaradaran-Esfahani. J. Alloys Compd. 830, 154588 (2020). Crossref

21. C. L. Yeh, M. C. Chen. Materials. 14, 4800 (2021). Crossref
22. Y. Sun, Y. Li, L. X. Zhang, L. Li, J. L. Sun. Ceram. Int. 46, 27774 (2020). Crossref
23. Q. Wu, G. Feng, F. Jiang, L. Miao, W. Jiang, J. Liang et al. Ceram. Int. 48, 3351 (2022). Crossref
24. G. P. Panasyuk, I. V. Kozerozhets, M. N. Danchevskaya, Y. D. Ivakin, G. P. Murav'eva, A. D. Izotov. Dokl. Chem. 487, 218 (2019). Crossref
25. F. Marais, I. Sigalas, D. Whitefield. Ceram. Int. 48, 563 (2022). Crossref
26. Y. X. Zhang, J. F. Wu, Y. Zhou, X. H. Xu, K. Z. Tian, Y. Liu. Ceram. Int. 47, 25081 (2021). Crossref
27. L. H. Liu, K. Morita. J. Eur. Ceram. Soc. 42, 2487 (2022). Crossref
28. Y. A. Liu, J. Q. Zhu, B. Dai. Ceram. Int. 46, 25738 (2020). Crossref
29. P. M. Bazhin, E. V. Kostitsyna, A. M. Stolin, A. M. Chizhikov, M. Ya. Bychkova, A. Pazniak. Ceram. Int. 45, 9297 (2019). Crossref
30. L. H. Lv, G. Xiao, D. Ding, Y. Ren, S. Yang, P. Yang et al. Int. J. Appl. Ceram. Technol. 16, 1253 (2019). Crossref
31. A. P. Chizhikov, P. M. Bazhin, A. M. Stolin. Lett. Mater. 10 (2), 135 (2020). (in Russian) Crossref
32. P. M. Bazhin, A. M. Stolin, M. I. Alymov, A. P. Chizhikov. Inorg. Mater. Appl. Res. 6, 187 (2015). Crossref
33. E. J. Minay, R. D. Rawlings, H. B. McShane. J. Mater. Process. Technol. 153, 630 (2004). Crossref
34. E. J. Minay, H. B. McShane, R. D. Rawlings. Intermetallics. 12, 75 (2004). Crossref
35. T. Gao, L. Y. Liu, J. P. Song, G. L. Liu, X. F. Liu. J. Alloys Comp. 868, 159283 (2021). Crossref
36. C. Freitas, N. Vitorino, M. J. Ribeiro, J. C. C. Abrantes, J. R. Frade. Appl. Clay Sci. 109, 15 (2015). Crossref
37. N. Vitorino, C. Freitas, M. J. Ribeiro, J. C. C. Abrantes, J. R. Frade. Appl. Clay Sci. 101, 315 (2014). Crossref
38. N. Vitorino, C. Freitas, M. J. Ribeiro, J. C. C. Abrantes, J. R. Frade. Appl. Clay Sci. 105, 60 (2015). Crossref
39. T. M. Vidyuk, M. A. Korchagin, D. V. Dudina, B. B. Bokhonov. Combust. Explos. Shock Waves. 57, 385 (2021). Crossref
40. N. Shaikh, K. Patel, S. Pandian, M. Shah, A. Sircar. Arab. J. Geosci. 12, 11 (2019). Crossref
41. P. M. Bazhin, E. V. Kostitsyna, A. P. Chizhikov, A. S. Konstantinov, L. E. Neganov, A. M. Stolin. J. Alloys Compd. 856, 157576 (2021). Crossref
42. A. P. Chizhikov, P. M. Bazhin, A. M. Stolin, M. I. Alymov. Dokl. Chem. 484, 79 (2019). Crossref
43. L. Lombardi, D. Tammaro. Phys. Fluids. 33, 033104 (2021). Crossref
44. J. N. Wang, T. Wang, J. Xu, J. C. Yu, Y. M. Zhang, H. P. Wang. J. Appl. Polym. Sci. 135, 8 (2018). Crossref